Pergamon

Int. J. Mach. Tools Manufact. Vol. 35, No. 3, pp. 363–372, 1995

0890–6955/95$9.50 + .00

0890–6955(94)E0028-H

ON THE MECHANISM OF COLD ROLLING THIN FOIL

L. C. ZHANG†

(*Received* 6 *January* 1993; *in final form* 7 *March* 1994)

Abstract—The deformation mechanism of cold rolling thin foil is investigated with the aid of the slab method in conjunction with an incremental analysis. The interaction between the rolls and foil is explored thoroughly. The effects of initial thickness and yield stress of foil materials are discussed in detail. Extensive numerical studies show that the pressure and shearing force profiles in the rolling bite vary significantly with the increment of reduction ratio. The distribution of slip and no-slip zones is much more complex than that predicted previously. In the regime of rolling extremely thin foils with a constant reduction ratio, the rolling load increases and the rolling torque decreases monotonically with decreasing inlet foil thickness. It is found, however, that the change of the central elastic/plastic no-slip zones has very little effect on the resultant rolling forces.

NOMENCLATURE

A_0, A_1	absolute values of non-dimensional coordinates of entry and exit contact points of the rolling bite, defined as $a_0/(\mu R)$ and $a_1/(\mu R)$, respectively
a_0, a_1	absolute values of the coordinates of the entry and exit contact points, respectively
b	half-thickness of foil
b_0	inlet half-thickness of foil
D	constant, defined by equation (8)
$[D]_{ep}$	elastic–plastic matrix, see equation (5)
d	distance between a pair of surface points at x on foil and roll, see equation (6)
E	Young's modulus
E^*	plane strain Young's modulus, defined as $E/(1-\nu^2)$
H	non-dimensional initial thickness of foil, defined as $2b_0\ E_R^*/(\mu RY)$
H'	tangential modulus of the uniaxial tensile curve of foil
L	ratio of the total length of no-reduction zones to that of the rolling bite
p	normal interface pressure between the foil and roll surfaces
Q	non-dimensional rolling torque, defined by equation (14)
q	shearing interface force between the foil and roll surfaces
R	radius of roll
r	reduction ratio
s_x, s_z, s_{xz}	stress deviations, see equation (5)
W	non-dimensional rolling load, defined by equation (14)
w^R, w^F	normal deflections of roll and foil surfaces, respectively
x,z	coordinates, see Fig. 1
Y	yield stress of foil

Greek symbols

β	central angle of a pressure element, see equation (8)
ϵ_x, ϵ_z, γ_{xz}	strains
θ	central angle, a variable
μ	friction coefficient
ν	Poisson's ratio
σ_x,σ_z,τ_{xz}	stresses

Superscripts and subscripts

b	back tension
F	foil
f	front tension
(i)	element index
(J)	inlet element indication
(K)	outlet element indication
R	roll

†Department of Mechanical and Mechatronic Engineering, The University of Sydney, Sydney, NSW 2006 Australia.

1. INTRODUCTION

PRECISE knowledge of the deformation mechanism of foil is essential for an efficient design and utilization of foil rolling mills. Fundamental studies have revealed that conventional theories of cold rolling are not satisfactory for describing the process of rolling thin foil. The problems are that these theories either neglect elastic deformation of the rolls or assume that the deformed roll surfaces remain circular arcs of an enlarged radius given by the Hitchcock formula. Furthermore, the critical assumption that slip occurs throughout the bite except at the neutral section is no longer valid in the regime of thin foil rolling. Hence, when applied to thin gauges, these theories propose that there is a limiting gauge below which reduction cannot be achieved; increasing the roll load flattens the rolls elastically without causing yield of the strip [1]. Our previous research (FJMZ method [1]) shows that the deformation mechanism of a foil in the rolling gap varies with the change of the entry foil thickness and reduction ratio. The Newton–Raphson method was applied to adjust the boundary positions between slip and no-slip, reduction and no-reduction and elastic and plastic deformation zones, which were specified by a set of equations and boundary conditions derived from a pre-analysis of mechanics. However, much computation effort is usually needed because of the complicated distribution of deformation zones. The finite element method is also inefficient in dealing with such a particular problem [2]; much more computer time is required compared with the FJMZ method.

The present paper investigates the mechanism of foil rolling in a more straightforward way. The slab method is used in conjunction with the incremental theory of plasticity. A study is carried out based on the fact that any point in foil material would experience loading–unloading processes during its travel through the rolling bite from the entry to the exit. Hence, a state of any physical quantities of a point in the foil, including stress and deformation, could be obtained by adding a new increment based on the last state. A simple algorithm for determining the interaction behaviour between rolls and foil is constructed. An overall discussion on the contact pressure, reduction ratio of foil, effect of entry foil thickness, yield stress, and the detailed diagram of elastic–plastic transition of the deformation zones in the contact arc is conducted. Extensive numerical analyses show that the actual deformation mechanism of foil is much more complex than that predicted previously. It is found, however, that the change of the central elastic/plastic no-slip zones has very little effect on the resultant rolling forces.

2. FORMULATION OF THE NEW ALGORITHM

2.1. *Basic equations*

When the foil inside the rolling contact region is divided into N slab elements, as shown in Fig. 1, the physical quantities in the $(i+1)$th element, such as stresses, strains, etc. could be expressed as

$$\begin{cases} \sigma_x^{(i+1)} = \sigma_x^{(i)} + \delta\sigma_x^{(i)}, & \sigma_z^{(i+1)} = \sigma_z^{(i)} + \delta\sigma_z^{(i)} \\ \epsilon_x^{(i+1)} = \epsilon_x^{(i)} + \delta\epsilon_x^{(i)}, & \epsilon_z^{(i+1)} = \epsilon_z^{(i)} + \delta\epsilon_z^{(i)} \\ b^{(i+1)} = b^{(i)} + \delta b^{(i)}, & q^{(i+1)} = q^{(i)} + \delta q^{(i)}, \end{cases} \tag{1}$$

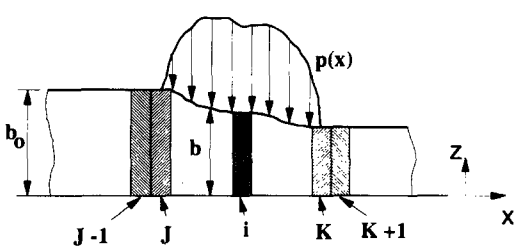

FIG. 1. Division of slab elements.

where $\delta(\ldots)$ stands for an increment of the quantity $(\ldots)$. Hence, the equilibrium equation of the foil in incremental form is given by

$$\delta b^{(i)} \frac{\mathrm{d}\sigma_x^{(i)}}{\mathrm{d}x} + (b^{(i)} + \delta b^{(i)}) \frac{\mathrm{d}\delta\sigma_x^{(i)}}{\mathrm{d}x} + (\delta\sigma_x^{(i)} + \delta p^{(i)}) \frac{\mathrm{d}b^{(i)}}{\mathrm{d}x} + [(\sigma_x^{(i)} + \delta\sigma_x^{(i)}) + (p^{(i)} + \delta p^{(i)})] \frac{\mathrm{d}\delta b^{(i)}}{\mathrm{d}x} + \delta q^{(i)} = 0. \tag{2}$$

Assume that the foil is in a plane-strain state; then the geometrical relation between the vertical strain and the foil thickness is

$$\delta\epsilon_z^{(i)} = \frac{\delta b^{(i)}}{b}. \tag{3}$$

If the foil material obeys an isotropic work hardening law after its first yielding, the stress–strain relations could be given by

$$[\delta\sigma] = [D]_{\mathrm{ep}}[\delta\epsilon], \tag{4}$$

where

$$[\delta\sigma] = (\delta\sigma_x, \delta\sigma_z, \delta\tau_{xz})^T$$

$$[\delta\epsilon] = (\delta\epsilon_x, \delta\epsilon_z, \delta\gamma_{xz})^T$$

$$[D]_{\mathrm{ep}} = \begin{pmatrix} \frac{1-\nu}{1-2\nu} - \eta s_x^2 & \frac{\nu}{1-2\nu} - \eta s_x s_z & -\eta s_x s_{zx} \\ \frac{\nu}{1-2\nu} - \eta s_x s_z & \frac{1-\nu}{1-2\nu} - \eta s_z^2 & -\eta s_z s_{zx} \\ -\eta s_x s_{zx} & -\eta s_z s_{zx} & \frac{1}{2} - \eta s_{zx}^2 \end{pmatrix}$$

$$\eta = \frac{9G}{2\bar{\sigma}^2(H' + 3G)}, \quad G = \frac{E}{2(1+\nu)}, \tag{5}$$

where $H' = E_{\mathrm{p}}$ is the tangential modulus of the uniaxial tensile curve of the foil material. For elastic–perfectly plastic materials, $H' = 0$. In equation (5), s_x, s_z and s_{zx} are stress deviations and $\bar{\sigma}$ is the effective stress.

2.2. *Compatibility of normal deflection between foil and roll surfaces*

Let d be the distance between a pair of surface points at x on foil and roll. Then

$$d = w^{\mathrm{R}} + w^{\mathrm{F}} + \zeta - \alpha, \tag{6}$$

where w^{R} and w^{F} are the normal surface deflection of the roll and that of foil at x, respectively, ζ is the initial distance between the two points before deformation and α is the rigid body displacement of the roll centre (in z-direction, see Fig. 1). Provided the contact length is small compared with the radius of the rolls, R, equation (6) could be rewritten as

$$d = b_0 - b + w^{\mathrm{R}} + \frac{x^2}{2R} - \alpha. \tag{7}$$

Consequently, $d^{(i)} > 0$ represents no-contact between the roll and foil at point i, $d^{(i)}$

$= 0$ denotes their contact but $d^{(i)} < 0$ should never happen because any material penetration between the two surfaces must not occur. As is well known, the contribution of shearing stress $q(x)$ to the roll surface deflection is negligible [3]. Thus the normal surface deflection relative to the roll centre, $w^R(x)$, can simply be calculated by

$$w^{R(i)} = \sum_{j=1}^{N} (w)_j^{(i)} p_j \qquad (i = 1, \ldots, N), \tag{8a}$$

where

$$w = \begin{cases} w^*, & |\theta| > \beta \\ w^* - \dfrac{R}{E}(1 - \nu_R - 2\nu_R^2), & |\theta| < \beta \end{cases} \tag{8b}$$

and

$$w^* = \frac{D}{\pi E}(1 - \nu_R^2)\left[\frac{x}{D}\ln\left(\frac{\dfrac{x}{D} + 1}{\dfrac{x}{D} - 1}\right)^2 + \ln\left(\frac{x^2}{D^2} - 1\right)^2 + \ln\left(\frac{\beta^2}{4}\right)^2\right]. \tag{8c}$$

In deriving the above expressions, we have assumed that the normal pressure $p(x)$ on the roll surface could be approximated by a set of uniformly distributed pressure $p^{(j)}$ $(j = 1, \ldots, N)$ over an arc element with a central angle 2β. In equation (8c), D is equal to $R\beta$ and is set to be the half-length of a slab element.

2.3. *Determination of interface shearing force* q(x)

A non-linear model is used to simulate the interface shearing force (see Fig. 2). In a slip region between the foil and rolls, the frictional traction $q(x)$ is related to the normal pressure by the Coulomb friction law:

$$q(x) = \gamma\mu p(x), \tag{9}$$

where $\gamma = +1$ when the foil is moving slower than the rolls and $\gamma = -1$ when it is moving faster. In a no-slip region, however, the foil and the roll surface move with the same speed. This indicates that the difference of tangential strains of the rolls and foil is constant, i.e.

$$\epsilon_x^R(x) - \epsilon_x(x) = \text{constant}.$$

Consequently,

$$\delta\epsilon_x^R(x) - \delta\epsilon_x(x) = 0. \tag{10}$$

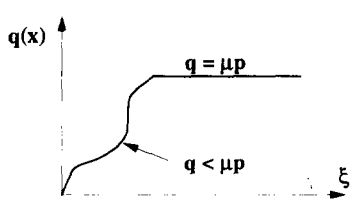

FIG. 2. The friction law (ξ is the creep coefficient, defined as the ratio of the relative slip speed of the roll and foil surfaces to the roll surface speed).

For the sake of convenience, we now assume that the tangential surface strain of rolls could approximately be determined by [3]

$$\epsilon_x^R = C_1 \frac{dq}{dx} + C_2 p, \tag{11}$$

where

$$C_1 = -\frac{9\pi a_0(1-\nu_R^2)}{16E_R}, \quad C_2 = -\frac{(1-2\nu_R)(1+\nu_R)}{E_R}.$$

Therefore

$$\delta\epsilon_x^R = C_1 \frac{d\delta q}{dx} + C_2 \delta p.$$

Hence according to equation (10),

$$\frac{d\delta q}{dx} = \frac{1}{C_1}(\delta\epsilon_x(x) - C_2\,\delta p(x)), \tag{12}$$

which specifies $q(x)$ when $|q|$ is less than $\mu p(x)$, as illustrated by the non-linear curve in Fig. 2.

2.4. *Entry and exit conditions*

Let the number of the entry contact element be J and that of the exit contact element be K. The conditions for determining entry and exit elements are then given by

$$\begin{aligned} &\sigma_x^{(J)} = \sigma_b, p^{(J)} = 0, q^{(J)} = 0, d^{(J)} = 0; \\ &\sigma_x^{(K)} = \sigma_f, p^{(K)} = 0, q^{(K)} = 0, d^{(K)} = 0. \end{aligned} \tag{13}$$

2.5. *The algorithm*

The assembly of equations (1)–(13) leads straightforwardly to a simple iteration scheme:

(a) specify the rigid body displacement of the roll centre, α;
(b) determine entry and exit contact points according to conditions (13);
(c) compute $b(x)$ by equation (7);
(d) with obtained b, calculate stresses with the aid of equations (2)–(5) and (9)–(12);
(e) check accuracy, if satisfied execute the next step, otherwise return to (b);
(f) calculate the non-dimensional rolling load and torque by

$$W = \frac{E_R}{RY^2(1-\nu_R^2)} \cdot \int_{-a_0}^{a_1} p(x)\,dx$$

$$Q = \frac{E_R^2}{R^2Y^3(1-\nu_R^2)^2} \cdot \left\{ \int_{-a_0}^{a_1} xp(x)\,dx + (\sigma_b b^{(J)} - \sigma_f b^{(K)})R \right\}; \tag{14}$$

(g) stop.

3. RESULTS AND DISCUSSION

3.1. *Rolling mechanism*

The variations of the normal and shearing contact forces with the increment of reduction ratio, r, are examined. Figure 3 shows that when r is small, say 12%, the

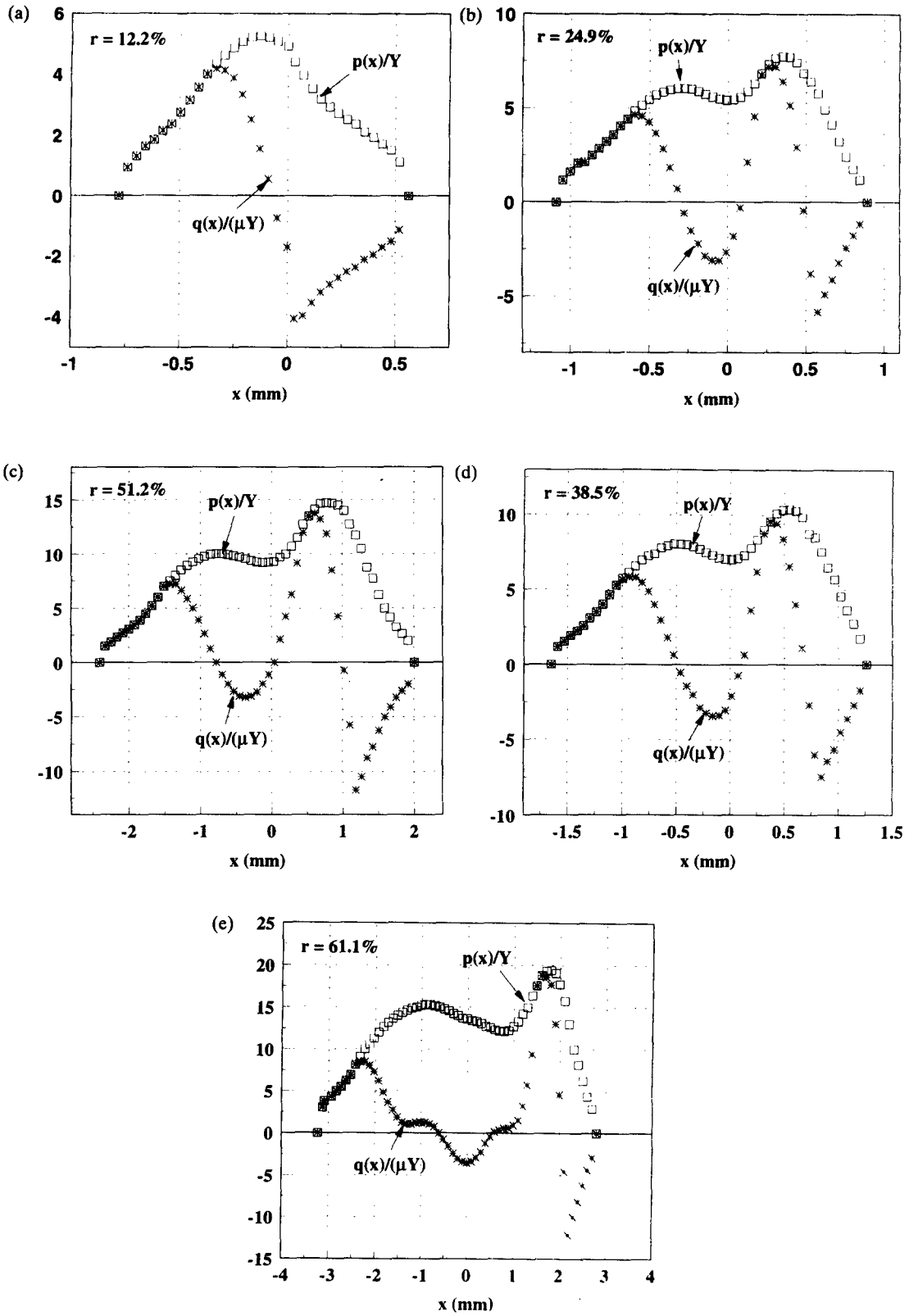

FIG. 3. The distribution of interface forces (b_0 = 0.01 mm, R = 89 mm, E_R = 210 GPa, E_s = 70 GPa, Y = 230 MPa, H' = 0, ν_R = 0.3, ν = 0.3, μ = 0.03, $\sigma_f = \sigma_b$ = 0).

normal pressure $p(x)$ distributes like a hill, which is very similar to that predicted by conventional theories in plate rolling (e.g. [4–6]). However, the present solution of foil possesses a no-slip zone at the central region which separates the reduction zone into two, one at the entry side and the other at the exit side. As r increases, the pressure profile changes to a double-peak pattern and then keeps this pattern for all the large reduction ratios. Besides the entry and exit slip regions, a small inverse slip zone, next to the central no-slip region, is observed when r goes beyond 15%. This could be recognized by the curves of $p(x)/Y$ and $q(x)/(\mu Y)$ where they coincide again in a very short interval after the separation by the central no-slip zones. Following this inverse slip, there always comes another narrow region of no-slip [see for example Fig. 3(b)], which is different from the prediction of the FJMZ model and shows that the transition of q from $+\mu p(x)$ to $-\mu p(x)$ is continuous in this narrow band.

Pressure peaks are neither sharp nor narrow, by contrast with the FJMZ's demonstration [1]. The shearing force changes more smoothly as well. The behaviour of the shearing force indicates that the transition from slip to no-slip is gradual and continuous and vice versa. They are characterized by the continuity of slopes of $p(x)$ and $q(x)$ curves. Furthermore, the variation of $q(x)$ is rather complex. For small reduction ratios [see Fig. 3(a)], it transfers straightforwardly from backward-slip friction at the entry side to forward-slip friction at the exit side. For the reductions between 15 and 55%, $q(x)$ shows two zones of inverse slip with a central zone of forward no-slip. When r exceeds 61%, the curve of the shearing force presents long flat shoulders near the zero line, which implies that the foil and roll surfaces in the central area are moving together with very small friction and that the contribution to ϵ_x^R there is mainly from $p(x)$, according to equation (11).

The above interface behaviour relates to the elastic–plastic deformation of the foil material. Figure 4 demonstrates the details of the deformation zones of the foil in the rolling bite. Clearly, the foil material experiences complex loading–unloading processes when it travels from the entry to the exit. Results show that the main reduction is obtained at the entry backward- and exit forward-slip regions. In the central area, the existence of elastic and plastic no-slip zones may vary from case to case: without any central elastic zone when $r < 15\%$, with one when $15 < r < 38\%$, two when $38 < r < 61\%$ and three when $r > 61\%$. Evidently, the transitions from elastic to plastic or from plastic to elastic deformation will change the values of $q(x)$ locally because it changes the longitudinal strains. However, as the overall profiles of pressure $p(x)$ and shearing force $q(x)$ as well as the length of the contact arc do not vary much with the distribution of the central no-reduction zones, they have only a tiny effect on the

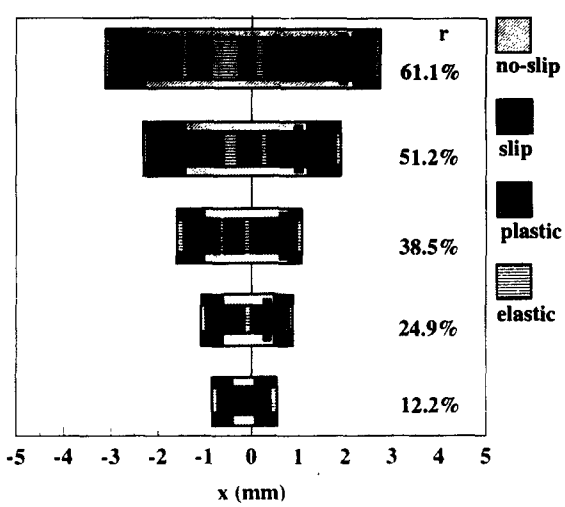

FIG. 4. Deformation zones inside the rolling gap.

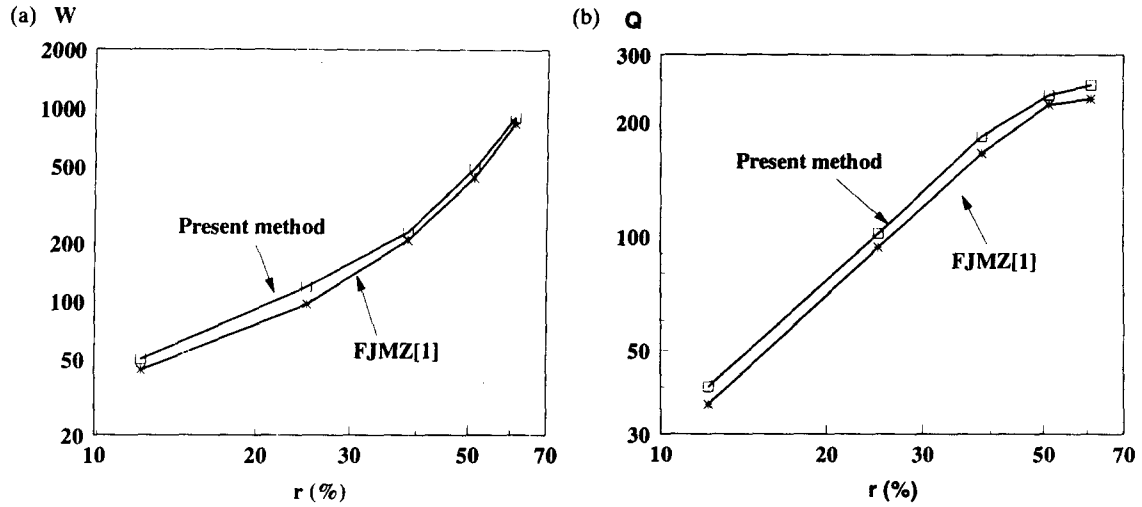

FIG. 5. A comparison of rolling load and torque. (a) Non-dimensional load. (b) Non-dimensional torque.

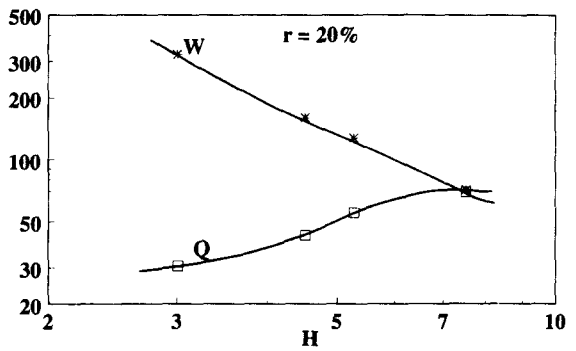

FIG. 6. Effect of entry foil thickness on the resultant rolling forces.

resultant rolling load and torque. This is confirmed well by comparison of the present results with those predicted by the FJMZ model (see Fig. 5). From the point of view of engineering application, therefore, it would be reasonable to divide the zones into two principal categories: reduction and no-reduction zones.

3.2. *Effect of entry foil thickness*

To examine the effect of the entry foil thickness, a constant reduction ratio is maintained throughout the analyses in Figs 6 and 7. The behaviour of foil deformation in large thickness regimes is simple and has been discussed extensively (e.g. [1, 4–6]).

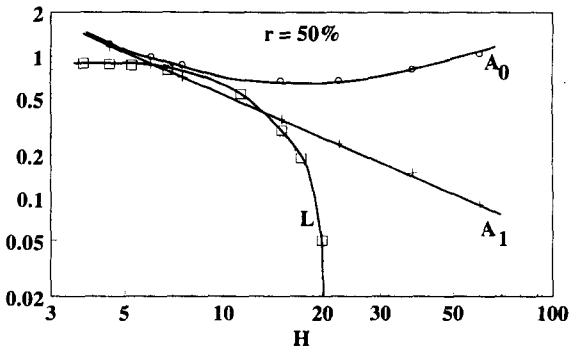

FIG. 7. Variations of the entry and exit contact points and the lengths of rolling zones.

The present discussions therefore focus on the rolling in the regime with extremely thin entry gauges.

The rolling load increases but the rolling torque decreases monotonically with the decrease of the entry foil thickness, as shown in Fig. 6, where $H = 2b_0E_R^*/(\mu RY)$ is the non-dimensional entry foil thickness. This could be explained by the variation of deformation zones shown in Fig. 7. When H becomes smaller and smaller, the inlet and outlet contact points approach symmetrical positions with respect to the origin $x = 0$, the central line of rolls. This means that the distribution of the rolling pressure profile becomes more symmetrical when H decreases. As a result, according to equation (14), Q decreases and W increases. It appears in Fig. 7 that the absolute values of non-dimensional coordinates of the inlet and outlet contact points, A_0 and A_1, approach each other when the entry foil thickness decreases. However, they will never meet because the curves of A_0 and A_1 run in parallel as H becomes less than 5. This indicates that the contribution of rolling pressure $p(x)$ to the rolling torque will never be zero regardless of how small H is.

The variation of the ratio of the total length of no-reduction zones to that of the whole rolling arc, L, yields an important prediction from a new angle (see Fig. 7). The fact that L approaches to a constant less than a unit states that there always exist reduction zones and hence there is not a limiting gauge as predicted by conventional theories.

3.3. *Effect of yield stress*

The yield stress of foil material affects all outcomes of a rolling operation. Figure 8 shows the variation of rolling load and torque as well as the reduction ratio and outlet contact point. The relative length of reduction zones decreases with increasing Y and accordingly the reduction ratio drops down remarkably. It is in good agreement with practical observations because the material subjected to rolling is getting harder when Y rises. Similar to the entry thickness effect discussed above, higher Y makes the rolling arc more symmetrical with respect to the central line of rolls. This is implied by the increasing value of A_1/A_0 as well as the reduction of the rolling torque. It may be unexpected that the rolling load decreases when the material becomes harder. However, the total rolling load is an integration of the pressure profile that depends on the detailed deformation of the foil in the rolling bite. Although a large Y value enlarges the length of the rolling bite, it lowers the mean level of $p(x)$ at the same time.

4. CONCLUSIONS

1. The deformation mechanism of foil in the rolling bite is carefully discussed. Reduction ratio is a major factor when the entry thickness of foil is given. For small

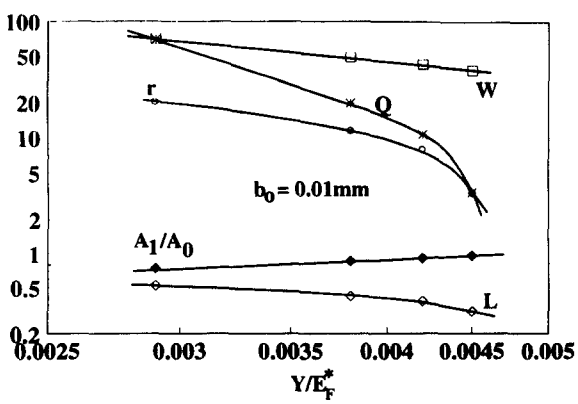

FIG. 8. Effect of yield stress.

reduction ratios, there exists only a plastic no-slip central zone, but for large ratios elastic regions grow out.

2. A small inverse slip zone emerges when the reduction ratio exceeds 15%. It is always followed by a no-slip plastic region which makes the transition of $q(x)$ from $+\mu p(x)$ to $-\mu p(x)$ continuous.

3. The profiles of pressure and shearing force vary smoothly and their slopes are continuous.

4. The details of the central zones have only little effect on the resultant rolling forces; thus the simplification algorithm proposed by [1] is reliable in this sense.

5. In the regime of rolling extremely thin foils, the rolling bite is almost symmetrical with respect to the central line of rolls. There always exist reduction zones and hence the contribution of $p(x)$ to the total rolling torque will never be zero.

6. With a given entry thickness and inlet contact point, the most direct effect of increasing yield stress is a remarkable decrease of the reduction ratio and rolling torque.

REFERENCES

[1] N. A. FLECK, K. L. JOHNSON, M. MEAR and L. C. ZHANG, Cold rolling of foil. *Proc. Inst. Mech. Engrs Part B: J. Engng Manufact.* **206**, 119–131 (1992).
[2] P. GRATACOS, P. MONTMITONNET, C. FROMHOLZ and J. L. CHENOT, A plane-strain elasto-plastic finite-element model for cold rolling of thin strip. *Int. J. Mech. Sci.* **34**(3), 195–210 (1992).
[3] K. L. JOHNSON, *Contact Mechanics*. Cambridge University Press, Cambridge (1985).
[4] T. VON KARMANN, Beitrag zür theorie des Walzvorganges. *Z. angeur. Math. Meth.* **5**, 139 (1925).
[5] E. OROWAN, Graphical calculation of roll pressure with the assumptions of homogeneous compression and slipping friction. *Proc. Inst. Mech. Engrs* **150**, 141 (1943).
[6] D. R. BLAND and H. FORD, The calculation of roll force and torque in cold strip rolling with tensions. *Proc. Inst. Mech. Engrs* **159**, 144 (1948).